Polymer Journal (2019) 51:1063–1071
https://doi.org/10.1038/s41428-019-0222-3

ORIGINAL ARTICLE

Chiroptical properties of reporter-modified or reporter-complexed highly 1,6-glucose-branched β-1,3-glucan

Koichi Tamano[1] · Kotoe Nakasha[2] · Mie Iwamoto[1] · Munenori Numata[3] · Toshio Suzuki[4] · Hiroshi Uyama[1] · Gaku Fukuhara[2,5]

Received: 18 April 2019 / Revised: 23 May 2019 / Accepted: 28 May 2019 / Published online: 19 June 2019

Abstract

The macromolecular structure of highly 1,6-glucose-branched β-1,3-glucan (**6BG3**) was elucidated spectroscopically by modification and complexation with chromophoric reporters. The circular dichroism spectra of 4-(dimethylamino)benzoic acid (DABz)-modified **6BG3** showed a relatively small but obvious bisignate couplet in an aqueous DMSO solution; however, in DMSO, **6BG3** forms a random coil. These chiroptical properties and the AFM images revealed that reporter-modified **6BG3** goes through a random coil-to-globule conversion process upon solvent switching. The macromolecular structure of native, nonchromophoric **6BG3** was further examined by complexation with 2,5-poly(3-(6-pyridiniohexyl)thiophene) (PyPT) in situ. The **6BG3** random-coil strand complexed with PyPT to afford a heteroduplex with a small amount of a heterotriplex, showing a large exciton coupling for the π,π* transition of PyPT. The amount of the heteroduplex hybridization was enhanced at higher pH due to further complexation of single strands of partially deprotonated **6BG3** with free PyPT.

Introduction

Natural polymers, e.g., DNA and collagen, always have clear macromolecular structures, and they play important roles in biological activities [1–4]. Among these polymers, polysaccharides are highly abundant in nature; the macromolecular structures of amylose, which is present in starch, and of cellulose, which is in the primary cell wall of green plants, are very famous. Amylose is known to form left-handed single helices [5–9], and cellulose adopts an extended and rather stiff rod-like microfibril conformation due to the formation of multiple hydrogen bonds [10–13]. It is therefore noted that the elucidation of their macromolecular structures is of particular significance from not only scientific but also a practical point of view due to their use as one-dimensional building blocks in nanoarchitectures [14–16].

Of the many polysaccharides reported thus far, β-1,3-glucans are unique polysaccharides consisting of β-(1 → 3)-linked D-glucose units with or without branching glucose moieties. Among β-1,3-glucans, curdlan (Cur) is structurally the simplest, as it has a linear main chain without branching glucose moieties, while schizophyllan (SPG) has a 1,6-linked glucose sidechain on the center unit of the repeating three-glucose unit in the main chain (Fig. 1). From a macromolecular perspective, one of the most intriguing features of Cur and SPG is that they are capable of reversibly denaturing to random coil and renaturing to a

Supplementary information The online version of this article (https://doi.org/10.1038/s41428-019-0222-3) contains supplementary material, which is available to authorized users.

✉ Hiroshi Uyama
uyama@chem.eng.osaka-u.ac.jp

✉ Gaku Fukuhara
gaku@chem.titech.ac.jp

[1] Department of Applied Chemistry, Osaka University, 2-1 Yamada-oka, Suita 565-0871, Japan

[2] Department of Chemistry, Tokyo Institute of Technology, 2-12-1 Ookayama, Meguro-ku, Tokyo 152-8551, Japan

[3] Department of Biomolecular Chemistry, Graduate School of Life and Environmental Sciences, Kyoto Prefectural University, Shimogamo, Sakyo-ku, Kyoto 606-8522, Japan

[4] Research & Development Laboratory Fujicco, Co., Ltd., 6-13-4 Minatojima-nakamachi, Chuo-ku, Kobe, Hyogo 650-8558, Japan

[5] JST, PRESTO, 4-1-8 Honcho, Kawaguchi, Saitama 332-0012, Japan

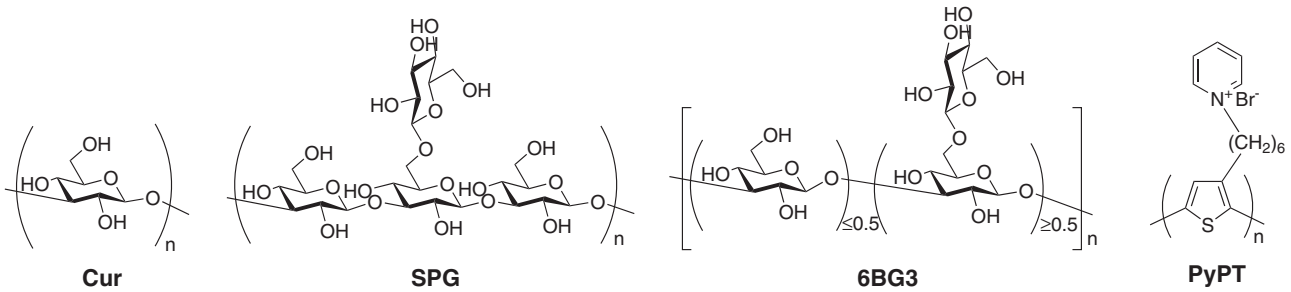

Fig. 1 Chemical structures of curdlan (Cur), schizophyllan (SPG), highly 1,6-glucose-branched β-1,3-glucan (**6BG3**), and pyridiniopolythiophene (PyPT)

triple helix by simply changing the solvent from DMSO or an aqueous alkaline solution to water or an aqueous acidic solution [17–22]. Another β-1,3-glucan reported relatively recently, highly 1,6-glucose-branched β-1,3-glucan (**6BG3**), i.e., over 50% glucose branching on the main chain as determined by sophisticated NMR techniques as shown in Fig. 1, was isolated from *Aureobasidium pullulans* 1A1 strain black yeast [23–27]. Most studies on **6BG3** have been devoted to elucidating its immunopharmacological activities [23–27]; nevertheless, the macromolecular structure of **6BG3** in solution has not been examined since spectroscopic studies on the macromolecular structure are inherently difficult due to the spectroscopically transparent characteristics of glucans in the typical UV-visible region. Therefore, the determination of the solution-state macromolecular structure of **6BG3** may facilitate further developments and advance our understanding of novel immune applications.

To indirectly avoid this inherent problem, we investigated the chiroptical properties of chromophore-modified Cur, and 4-(dimethylamino)benzoic acid (DABz) was chosen as the modification reporter. The chiroptical properties obtained from DABz-modified Cur (**DABz-Cur** shown in Fig. 2; with different degrees of substitution (DS), prepared as reported previously) revealed that the random coil of modified Cur in DMSO forms globules upon the addition of water instead of triple helices (see Fig. 5b) [28–31]. Since the random coil-to-globule conversion process is quite characteristic of modified Cur [30, 31], comparing the various data obtained using this modification strategy can be used to elucidate the macromolecular structure of **6BG3**. Furthermore, without modification of the glucan, the chiroptical properties of native, nonchromophoric Cur and SPG can be directly investigated using 2,5-poly(3-(6-pyridiniohexyl)thiophene) (PyPT, as shown in Fig. 1) as a chromophoric hybridization partner. The glucan in the form of random coil interacts with PyPT to give a heterotriplex of glucan/PyPT (2:1) by replacing one of the three glucan strands in the homotriplex, and the heterotriplex subsequently dissociates to the heteroduplex of glucan/PyPT (1:1) upon elevation of the pH [32, 33]. Therefore, the PyPT reporter can provide structural information on native glucans, i.e., homotriplex or homoduplex.

In the present study, we investigated the chiroptical properties of reporter-modified or reporter-complexed **6BG3**; thus, DABz (for modification) and PyPT (for hybridization) were chosen as UV-vis and circular dichroism (CD) spectroscopic reporters in the same manner. Hence, by comparing the chiroptical properties of **DABz-Cur** and the Cur/SPG-PyPT complexes [28–33], we could accurately determine the solution-state macromolecular structure of native, nonchromophoric **6BG3**. The present study (1) provides an easier synthetic protocol for directly conjugating a chromophore onto the backbone of a glucan, (2) elucidates the random coil-to-globule conversion process of reporter-modified glucans, which may be expanded to novel supramolecular hosts and drug delivery systems, and (3) demonstrates the dynamic hybridization of glucans, particularly for **6BG3**, with cationic polythiophene to ultimately indicate the solution-state macromolecular structures of glucans, which can provide deep insights into the factors controlling the macromolecular and spectroscopic properties of glucans.

Experimental procedure

Materials

Commercially available Cur and **6BG3**, supplied by DS Wellfoods Co., Ltd., were dried under high vacuum overnight at 60 °C prior to use. The degree of glucose branching of the **6BG3** employed in the present study was determined to be 0.90 by ^{1}H NMR spectroscopy according to a literature procedure [23–27] (see Fig. S1 in the Supplementary Information (SI)). The number-average molecular weight (M_n) and the polydispersity index (PDI) were determined to be 1300 kDa and 1.5 for Cur and 3300 kDa and 3.9 for **6BG3**, respectively. Regioregular head-to-tail 2,5-poly(3-(6-pyridiniohexyl)thiophene) (PyPT, reported previously [32]) was used. Spectrophotometric-grade DMSO and water (milli-Q) were used as solvents without further purification.

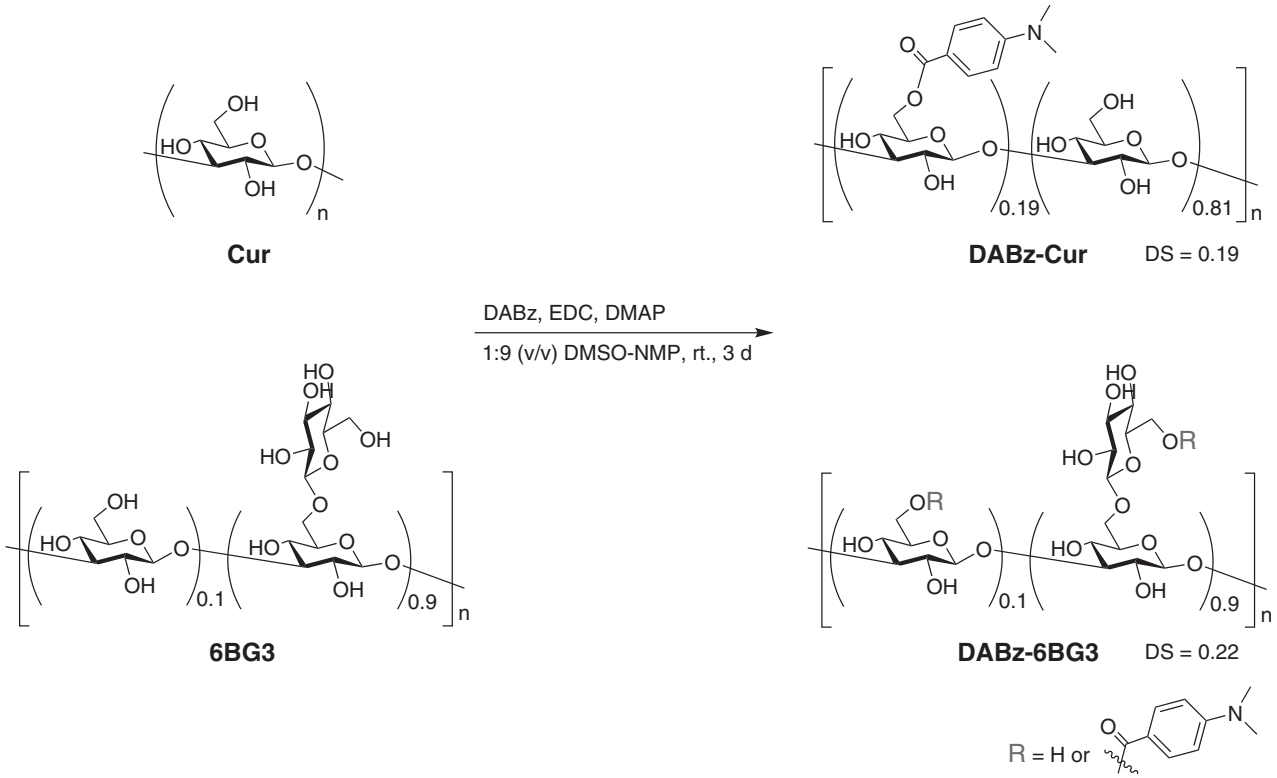

Fig. 2 Synthetic scheme of DABz-modified glucans

A 1:9 (v/v) DMSO-H_2O solution of glucans (at a concentration comparable to that used in the spectroscopic studies) was dropped onto a mica surface, and the residue was dried under flowing N_2 gas and then under a high vacuum to prepare it for atomic force microscopy (AFM) analysis.

Synthesis of DABz-Cur

The synthetic routes to both DABz-modified glucans are shown in Fig. 2. Native Cur (212 mg, 1.31 mmol based on monomer units) was placed in a flask and dissolved in dry DMSO (4 mL), and dry *N*-methyl-2-pyrrolidinone (NMP) (36 mL) was added under N_2. The resulting viscous solution was heated to 80 °C and stirred overnight at that temperature. After cooling to room temperature, DABz (45.3 mg, 0.274 mmol, 0.209 eq), *N*,*N*-dimethyl-4-aminopyridine (DMAP) (310 mg, 2.54 mmol), and 1-ethyl-3-(3-dimethylaminopropyl)carbodiimide hydrochloride (EDC) (502 mg, 2.62 mmol) were added to the Cur solution. The reaction mixture was stirred for 1 day at room temperature, and then the same amounts of DMAP and EDC were added twice per day as the reaction was continued for a total of 3 day. The reaction solution was slowly poured onto methanol (500 mL) to give a white precipitate, which was swelled in DMSO (45 mL) and stirred for 1 day at 83 °C. The resulting mixture was slowly poured onto methanol (500 mL) to give a white precipitate, which was collected, washed with methanol, and then dried under high vacuum to afford 6-*O*-(4-(dimethylamino)benzoyl)curdlan (**DABz-Cur**) in 51% yield (127 mg, 0.668 mmol with respect to the monomer unit) as a white solid. The degree of substitution (DS) was determined to be 0.19 by UV-vis spectrometry (see Fig. 3a and the relevant discussion). Since we have already reported the full assignments of **DABz-Cur** with 0.12 DS [28], the **DABz-Cur** with 0.19 DS thus obtained was only characterized by ^{1}H NMR spectroscopy as it only varied by its DS. ^{1}H NMR (DMSO-d_6, 400 MHz, room temperature) δ_H 7.84 (H_a), 6.70 (H_b), 5.19-3.16 (sugar protons), 3.00 (Me-N) (see Fig. S2).

Synthesis of DABz-6BG3

Native **6BG3** (217 mg, 0.704 mmol with respect to the monomer units) was placed in a flask and dissolved in dry DMSO (4 mL) at 70 °C, and dry NMP (36 mL) was added under N_2. The resulting viscous solution was heated to 90 °C and stirred overnight at that temperature. After cooling to room temperature, DABz (26.3 mg, 0.159 mmol, 0.226 eq), DMAP (180 mg, 1.47 mmol), and EDC (249 mg, 1.30 mmol) were added to the **6BG3** solution. The reaction mixture was stirred for 1 day at room temperature, and then the same amounts of DMAP and EDC were added twice per day as the reaction was continued for a total of 3 day.

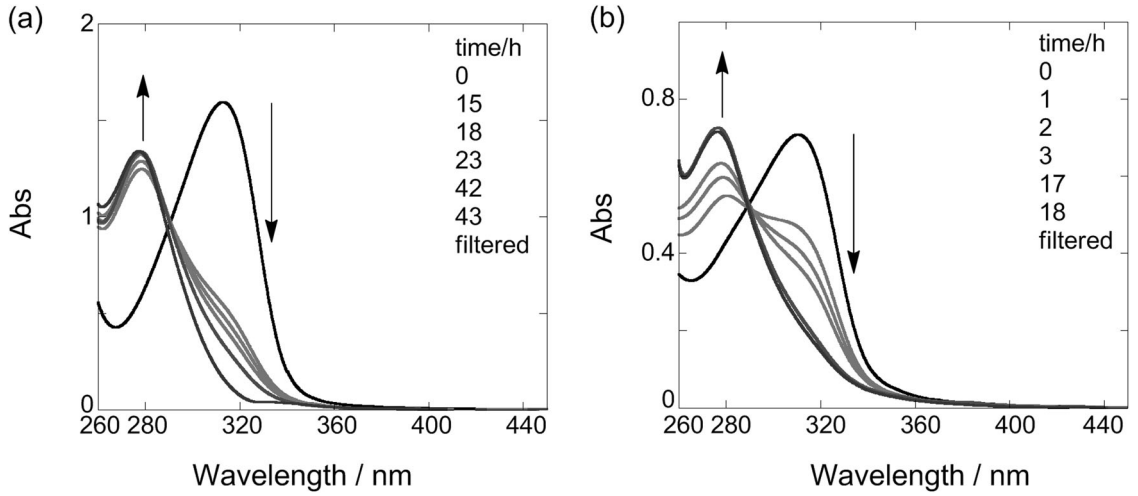

Fig. 3 Changes in the UV-vis spectra of **a DABz-Cur** and **b DABz-6BG3** in 5:95 (v/v) KOH aq-DMSO during hydrolysis (from black to blue)

The resulting mixture was slowly poured onto methanol (600 mL) to give a white precipitate, which was collected and centrifuged at 11,000 rpm for 10 min in methanol and then dried under high vacuum to afford 6-*O*-(4-(dimethylamino)benzoyl)**6BG3** (**DABz-6BG3**) in 64% yield (153 mg, 0.448 mmol in monomer unit) as a white solid. The DS was determined to be 0.22 by UV-vis spectrometry (see Fig. 3b and the relevant discussion). ^{1}H NMR (DMSO-d_6, 600 MHz, 40 °C) δ_H 7.79 (H_a), 6.72 (H_b), 5.22-3.04 (sugar protons), 3.00 (Me-N); ^{13}C NMR (DMSO-d_6, 150 MHz, 40 °C) δ_C 166.3 (C = O), 153.9 (C_c), 131.4 (C_a), 111.4 (C_b), 103.7 (C_1), 86.6 (C_3), 77.1, 76.9, 75.2, 74.2, 73.1, 70.7, 69.0, 61.6 (C_6), Me-N (overlapped with DMSO peak as determined from the HSQC spectrum) (see Fig. S3-4); IR (ATR) ν 3359, 2902, 1684, 1605, 1531, 1434, 1368, 1315, 1283, 1165, 1073, 1043, 903, 770, 655 cm^{-1}.

Results and discussion

Synthesis and characterization of DABz-modified glucans

Although sophisticated synthetic protocols for incorporating chromophores into glucans have been developed [20, 21], the direct modification/conjugation of chromophores onto glucan backbones with control of the DS is rather difficult due to the poor solubility of glucans, particularly Cur and **6BG3**. We have already reported an easy and direct modification of native Cur for synthesizing 6-*O*-(4-(dimethylamino)benzoyl)Cur (**DABz-Cur**) by the reaction of 4-(dimethylamino)benzoyl chloride with native Cur [28], and the swelling of native Cur in NMP prior to the reaction is the key to the success of this reaction. Herein, we synthesized **DABz-Cur** by a different esterification using EDC and DMAP in a mixture of DMSO-NMP (v/v 1:9) since **6BG3** does not dissolve in pure NMP, and hence, its esterification/purification should be compared to that of the **DABz-Cur** prepared herein. Thus, the esterification of **6BG3** followed the same synthetic procedure as that of **DABz-Cur**, using EDC/DMAP, as shown in Fig. 2. Comparing the NMR spectra of the **DABz-Cur** samples obtained from the present (EDC/DMAP) and previous (carboxylic chloride) synthetic methods confirmed the selective and highly efficient esterification of DABz at the 6-positions of the sugar skeleton. The obtained **DABz-6BG3** was characterized by 1D- and 2D-NMR spectroscopy (see Figs. S3 and S4 in the SI and Experimental Section), which confirmed the selective esterification at the 6-positions of the main chain and/or branching glucose moieties. Thus, the present synthetic method using EDC and DMAP in a DMSO-NMP mixture is substantially easier; it is not synthetically impressive, but it is effective for glucan modification, and it was better than the various reaction conditions examined to date.

The DS of DABz-modified glucans was determined by the comparison of the molar extinction coefficient of an authentic anionic DABz solution and to that of DABz liberated from the DABz-modified glucans upon hydrolysis in an aqueous alkaline solution using UV-vis spectroscopy (Fig. 3). For this analysis, **DABz-Cur** (5.58 mg) or **DABz-6BG3** (7.52 mg) was dissolved in DMSO (5 mL) to give the corresponding stock solutions. The stock solution of **DABz-Cur** (0.5 mL) was transferred to a 5-mL volumetric flask, and the solution was brought to 5 mL with DMSO. A 250-µL aliquot of this DMSO solution was taken and replaced with 250 µL of aqueous KOH (98.6 mM) to prepare a 5:95 (v/v) aqueous KOH-DMSO solution of **DABz-Cur** (0.106 mg mL^{-1}). On the other hand, 300 µL of the stock solution of **DABz-6BG3** was transferred to a 5-mL

volumetric flask, and the solution was brought to 4.75 mL with DMSO. Aqueous KOH (0.25 mL, 75.6 mM) was added to prepare a 5:95 (v/v) aqueous KOH-DMSO solution of **DABz-6BG3** (0.0902 mg mL^{-1}). The resulting mixtures were hydrolyzed for 43 h for **DABz-Cur** (Fig. 3a) or for 18 h for **DABz-6BG3** (Fig. 3b). A gradual increase in the anionic DABz absorbance at ~276 nm and a decrease in the original DABz ester absorbance at ~312 nm were observed by UV-vis spectroscopy. Upon completion of the hydrolyses at 43 h for **DABz-Cur** or 18 h for **DABz-6BG3**, the concentrations of the liberated DABz anion in the filtrates of the hydrolyzed **DABz-Cur** or **DABz-6BG3** were 6.60×10^{-5} M and 3.53×10^{-5} M, respectively, based on the molar extinction coefficient of the authentic anionic DABz solution at 276 nm. Since if the DS of **DABz-Cur** and **DABz-6BG3** are 1.0, the concentration of the liberated DABz anion should be 3.43×10^{-4} M for **DABz-Cur** and 1.58×10^{-4} M for **DABz-6BG3**, the DS for the compounds were calculated to be 0.19 ($= 6.60 \times 10^{-5}/3.43 \times 10^{-4}$) for **DABz-Cur** and 0.22 ($= 3.53 \times 10^{-5}/1.58 \times 10^{-4}$) for **DABz-6BG3**, as shown in Fig. 2.

Chiroptical properties and morphological features of DABz-modified glucans

The chiroptical properties of **DABz-6BG3** after modification with the reporter were examined with UV-vis and CD spectra in DMSO and an aqueous solution containing 10% DMSO, and the spectra were compared with those obtained from **DABz-Cur**. The CD spectrum of **DABz-Cur** measured in DMSO showed an extremely weak negative Cotton effect for the intramolecular charge-transfer (CT) of DABz [34] centered at 315 nm (Fig. 4a, black line), indicating that **DABz-Cur** forms random coil in DMSO. In sharp contrast, a negative exciton coupling was observed in the same region in 1:9 (v/v) DMSO-H_2O, and the amplitude of the exciton couplet was 17.7 M^{-1} cm^{-1} (Fig. 4a, red line), suggesting a left-handed helical alignment of the DABz reporters according to the exciton chirality theory [35]. We have recently revealed that chromophore-modified Curs in random-coil state in DMSO form globules instead of triple helices in aqueous DMSO solutions by direct observation using atomic force microscopy (AFM) [28–31], which may be a better method for elucidating the morphology of glucans [36]. Hence, these contrasting behaviors in DMSO and aqueous solutions were also observed in previous evaluations of the chiroptical properties of 0.12 and 0.11 DS's **DABz-Cur** [28, 31], indicating that higher (19%) modification of Cur by DABz reasonably preserves the random coil-to-globule conversion (see Fig. 5b).

Intriguingly, the CD signal of the CT band of **DABz-6BG3** in DMSO exhibited a very weak but positive exciton coupling, the crossover point of which corresponds to the UV maximum at 310 nm (Fig. 4b, black line), and **DABz-Cur** in DMSO was the system to show a negative Cotton effect in its CD spectrum (Fig. 4a, black line). Since **DABz-6BG3** is known to dissociate to a single strand in DMSO [23–27], DABz reporters that are close to each other and

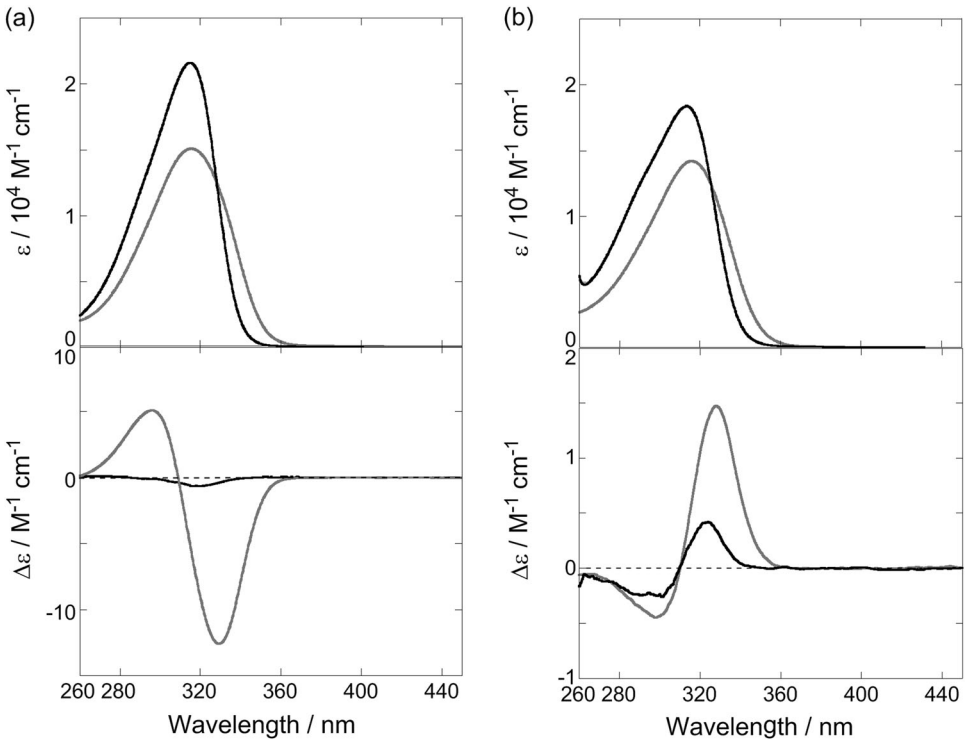

Fig. 4 UV-vis and CD spectra of **a** 113 μM (based on the chromophore unit) solutions of **DABz-Cur** and **b** 78.6 μM (based on the chromophore unit) solutions of **DABz-6BG3** in DMSO (black) and 1:9 (v/v) DMSO-H_2O (red), both measured in a 1-cm cell at 25 °C. Note that the molar extinction coefficient (ε) and molar ellipticity (Δε) were calculated by using the chromophore concentration (not the monomer units)

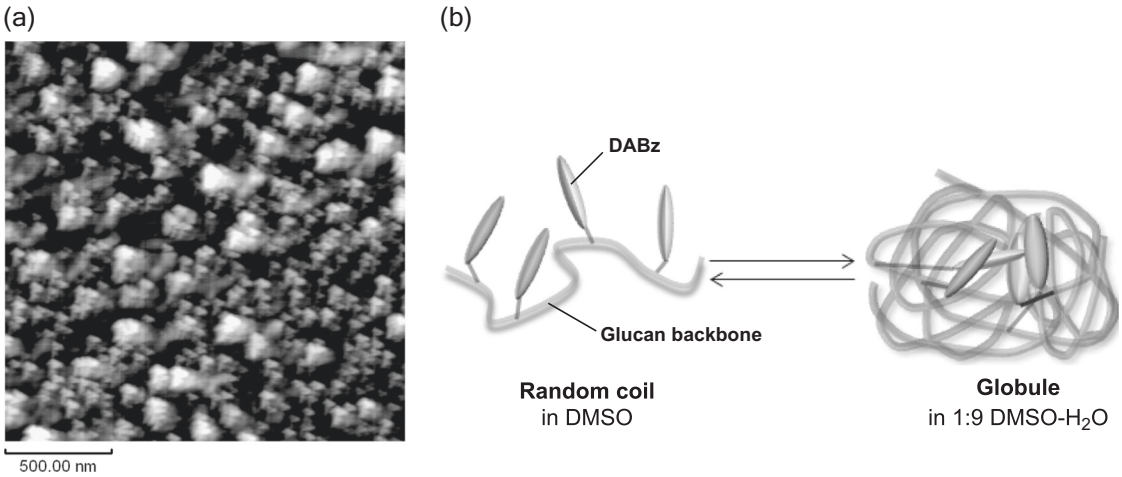

Fig. 5 **a** AFM image of **DABz-6BG3** prepared from its 1:9 (v/v) DMSO-H_2O solution on a mica surface. **b** Schematic of the reversible random coil-to-globule conversion of the DABz-glucan conjugates

movable interact with each other on the branching backbone bearing flexible glucose sidechains of **6BG3**, rather than direct DABz modification of the linear backbone of Cur. This behavior is confirmed by the hypochromic shift and band broadening in the UV spectrum of the DMSO solution of **DABz-6BG3** (full width at half maximum (fwhm) = 5320 cm^{-1}) that are observed relative to those of **DABz-Cur** (fwhm = 4390 cm^{-1}) (Fig. 4, black lines). In 1:9 DMSO-H_2O (Fig. 4b, red line), an obvious bisignate CD couplet was observed at the CT band. Nevertheless, its sign is opposite (right-handed arrangement) and its amplitude is 1.93 M^{-1} cm^{-1}, making it smaller than that of **DABz-Cur** by a factor of 9. To elucidate the differences in the chiroptical properties of these modified glucans in the aqueous DMSO solution, we investigated the morphological features of **DABz-6BG3** prepared from an aqueous DMSO solution. Thus, we analyzed an aqueous solution containing **DABz-6BG3** by AFM on a mica surface, and the images are shown in Fig. 5a and S5 (SI). The AFM image of **DABz-6BG3** showed many spots 107 ± 31 nm in diameter and 6.2 ± 2.7 nm in height, indicating that the random coil of the chromophoric **6BG3** in DMSO also goes through a random coil-to-globule conversion upon the addition of water into the DMSO solution containing **DABz-6BG3**, as illustrated in Fig. 5b, which is similar to that is seen with the modified Curs [28–31]. These results suggest that the reversible macromolecular features of **6BG3** are quite similar to those of Cur.

Returning to the chiroptical properties, the exciton coupling observed in **DABz-6BG3** in 1:9 DMSO-H_2O originates from the formation of **DABz-6BG3** globules during the conversion process, and hence, both the opposite sign and smaller amplitude of the CD signal are likely to be caused by the formation of looser globules, i.e., different chiral arrangements of the tethered reporters, rather than tight Cur globules, due to the large steric hindrance in the 90% branched glucose moieties on the **6BG3** main chain. Since the random coil-to-globule conversion process has been observed in supramolecular globule hosts [28–31], this finding may lead to the creation of novel glucan-based chemosensors and thus should attract the attention of a broad spectrum of not only macromolecular but also supramolecular chemists.

In situ hybridization of 6BG3 with PyPT

To further elucidate the macromolecular structure of **6BG3** more directly, we employed PyPT as a polymer reporter (Fig. 1) because it is known as a promising chromophoric tool for elucidating the macromolecular structures of β-1,3-glucans, i.e., Cur and SPG, which were recently reported [33]. As shown in Fig. 6a, PyPT showed a broad π,π* transition in the 350–600 nm region and essentially no CD signal (black dotted line), while upon complexation with Cur, PyPT exhibited a positive bisignate couplet in 1:9 DMSO-H_2O (pH 6.3; black solid line), which is indicative of the heterotriplex [PyPT•$(Cur)_2$] in which one of the Cur strands in the trimer has been replaced. Interestingly, the heterotriplex [PyPT•$(Cur)_2$] dissociates to a heteroduplex [PyPT•Cur], as indicated by the positive exciton coupling at longer wavelengths in 1:9 DMSO-H_2O at higher pH (pH 12.1; blue line), and at this pH, the UV intensity is reduced due to the partial precipitation of the PyPT species. The heterotriplex [PyPT•$(Cur)_2$] and heteroduplex [PyPT•Cur] were assigned based on the molar ratio plots. Thus, PyPT formed the heterotriplex upon complexation with glucans (Cur and SPG), and this complex dissociated to a loose heteroduplex at higher pH values (≥10.5) according to our recent report [33]. Interestingly, upon complexation with PyPT, even at pH 6.3, a 10% DMSO aqueous solution of

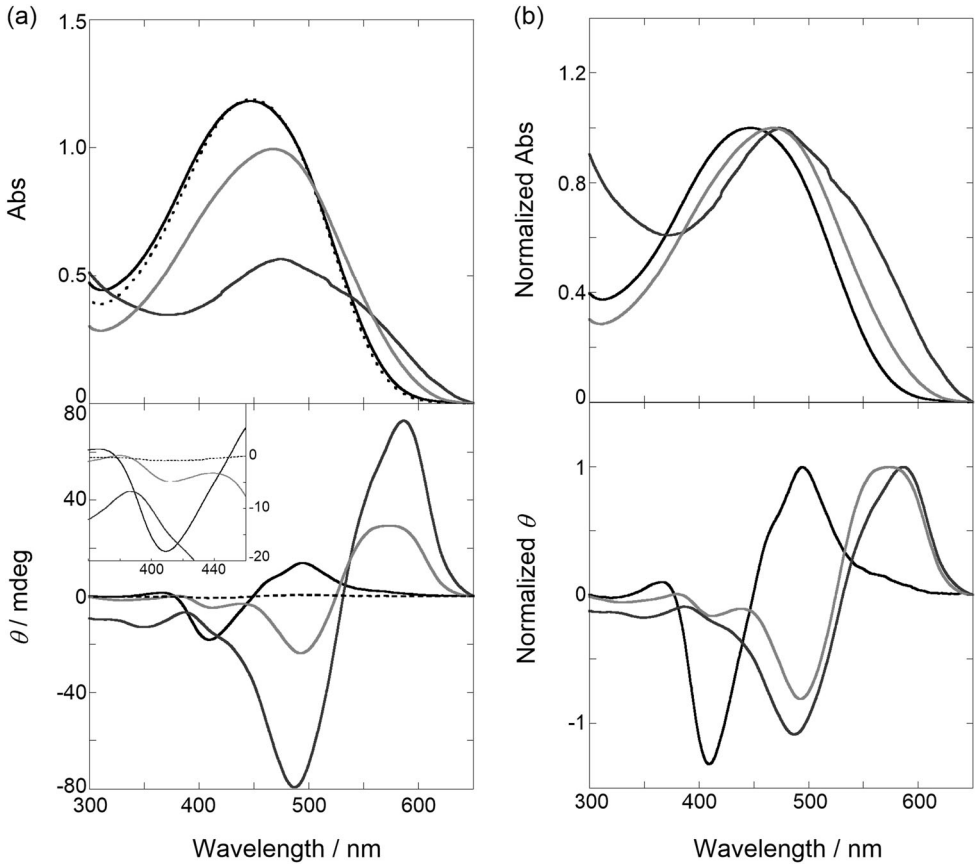

Fig. 6 **a** Regular and **b** normalized UV-vis (top) and CD (bottom) spectra of 0.2 mM PyPT in the absence (black dotted) and presence of 1.0 mM Cur (pH 6.3 as-prepared; black solid, pH 12.1; blue) (data from reference [33]) and 0.4 mM **6BG3** (pH 6.3 as-prepared; red) in a 1:9 (v/v) DMSO-H_2O solution at 25 °C in a 1-cm cell; all polymer concentrations are described based on the monomer units. The inset shows the expand spectrum

6BG3 (as prepared; red line) showed an obvious positive exciton coupling at longer wavelengths (450–650 nm) with a hypochromic effect and bathochromic shift in the UV-vis spectra compared to that obtained from the as-prepared Cur-PyPT solution (black solid line). In Fig. 6b, the CD peaks at 492 and 573 nm and the overall shape of the CD spectrum of the as-prepared **6BG3**-PyPT (red line) are quite similar to that of Cur-PyPT at pH 12.1 (blue line), which showed signals at 487 and 586 nm, indicating the formation of a heteroduplex [PyPT•**6BG3**]. These results suggest that PyPT replaces one of the **6BG3** strands to give the heteroduplex [PyPT•**6BG3**], and hence, **6BG3** tends to form the homoduplex rather than a homotriplex. Further important changes in the CD spectra of **6BG3** with PyPT were observed, confirming the presence of a very small amount of the [PyPT•(**6BG3**)$_2$] heterotriplex at 412 nm (red line), which corresponds to the heterotriplex [PyPT•$(Cur)_2$] at 409 nm (black solid line). Assuming that the exciton coupling intensity of the heterotriplex is likely to be larger than that of the same concentration of the heteroduplex since the chirality of the heterotriplex is more uniform than that of the heteroduplex, the ratio of the heterotriplex [PyPT•(**6BG3**)$_2$] to the heteroduplex [PyPT•**6BG3**] is smaller than the ratio of the CD peaks, as |-4.8 mdeg| (412 nm)/29.3 mdeg (573 nm) = 16%. From the macromolecular structural point of view, **6BG3** forms the heteroduplex [PyPT•**6BG3**] (>84%) and the heterotriplex [PyPT•(**6BG3**)$_2$] (<16%) upon complexation with PyPT, reflecting the behavior of native **6BG3**, which forms the homoduplex and a small amount of the homotriplex in aqueous DMSO solutions, as shown in Fig. 9. The formation of the "loose" homoduplex of **6BG3** is confirmed by the fact that modified **DABz-6BG3** in 10% DMSO aqueous solution forms looser globules than those formed by **DABz-Cur** in the same aqueous solution, which again, is due to the steric repulsion from the many branching glucose moieties on the main chain of **6BG3**. To further directly clarify the macromolecular structure, DMSO aqueous solutions of native Cur and **6BG3** were analyzed by AFM. As shown in Fig. 7 (left), the AFM image of native Cur shows a triple-stranded fibril, which is consistent with previous reports [30]. On the other hand, the image of native **6BG3** (Fig. 7, right) shows an obscure, dispersed, sheet-like structure probably due to the collapse of the loose duplex structure during the drying process on the mica.

Effect of pH

Higher pH levels facilitate the hybridization of glucans (Cur and SPG) with PyPT due to electrostatic interactions of the partially deprotonated glucans with positively charged

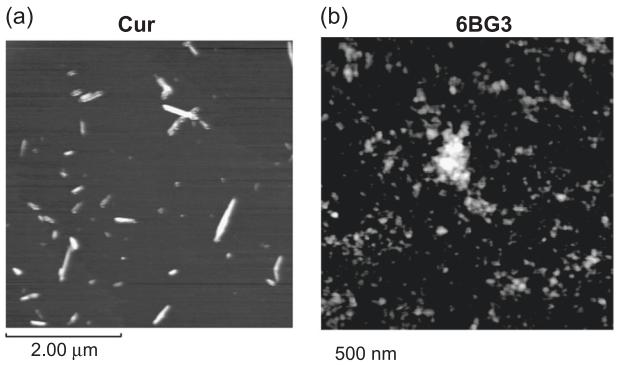

Fig. 7 AFM images of **a** native Cur and **b** native **6BG3** prepared from their 1:9 (v/v) DMSO-H_2O solutions on a mica surface

PyPT [33]. Thus, we next investigated the effect of pH on the hybridization of **6BG3** with PyPT using UV-vis and CD spectroscopies. As seen from the UV-vis spectra in Fig. 8, an obvious bathochromic shift of 10 nm was observed at pH 11.4 (red) and 12.1 (blue) compared to the as-prepared solution (black); however, the UV intensity was lower due to the partial precipitation of the PyPT species. In the CD spectra of Fig. 8b (bottom), the intensity of the peak at 412 nm, assigned to the heterotriplex [PyPT•(**6BG3**)$_2$], gradually decreased to a plateau of almost zero with increasing pH, and the exciton coupling intensity of the heteroduplex [PyPT•**6BG3**] increased with increasing pH since the effective UV intensities were reduced due to precipitation. These observations indicate that the amount of the heteroduplex increased due to the dissociation of more of the negatively charged single strand in the heterotriplex and subsequent complexation of the dissociated strand with a free PyPT species at pH ≥ 11.4, as shown in Fig. 9.

In the present study, we elucidated the solution-state macromolecular structure of **6BG3** by modification and complexation of chromophoric reporters. The reporter-**6BG3** conjugate does not form organized macromolecular structures and instead forms globules in an aqueous DMSO solution, as was the case with modified Curs, enabling us to use a reporter-**6BG3** conjugate as a supramolecular loose globule host that differs from the tight globules of Cur and SPG. Further supramolecular sensing applications based on the random coil-to-globule conversion process are currently being explored. The 90% branched **6BG3** derivative formed loose homoduplex structures, rather than tight the homotriplex observed in unbranched Cur and 33% branched SPG by a renaturing process in an aqueous DMSO solution due to the large steric repulsion of the high number of branching glucose moieties on the backbone. As was the case with Cur and SPG, the **6BG3** random-coil also complexes with PyPT in aqueous solutions to give the heteroduplex [PyPT•**6BG3**] and a small amount of the heterotriplex [PyPT•(**6BG3**)$_2$],

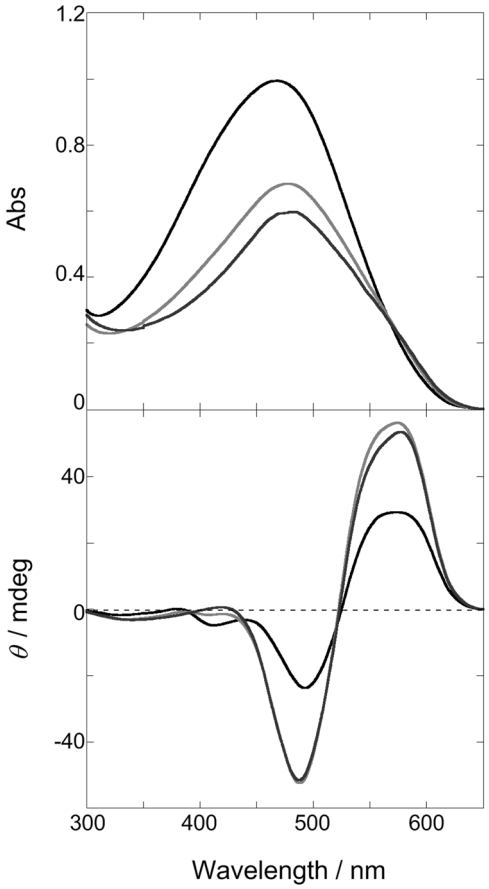

Fig. 8 UV-vis (top) and CD (bottom) spectra of 0.2 mM PyPT in the presence of 0.4 mM **6BG3** (pH 6.3 as-prepared; black, pH 11.4; red, pH 12.1; blue) in a 1:9 (v/v) DMSO-H_2O solution at 25 °C in a 1-cm cell; all polymer concentrations are described based on the monomer units

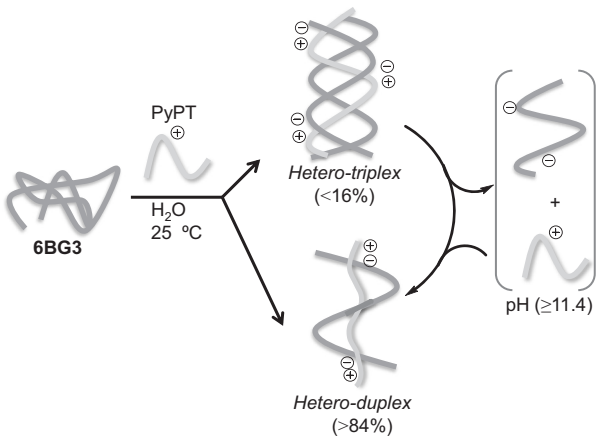

Fig. 9 Dynamic hybridization of **6BG3** with PyPT in situ

which further dissociates to the heteroduplex at higher pH. Thus, the uses of the PyPT reporter may be expanded to the elucidation of the macromolecular structures of other glucans and polysaccharides.

Acknowledgements We are deeply grateful to Prof. Yoshihisa Inoue of Osaka University for valuable suggestions. GF appreciates the generous support provided by a Grant-in-Aid for Young Scientists (A) (no. JP16H06041), Challenging Exploratory Research (no. 26620061) from the Japan Society for the Promotion of Science (JSPS) and Japan Science Technology Agency (JST), PRESTO (no. JPMJPR17PA).

Compliance with ethical standards

Conflict of interest The authors declare that they have no conflict of interest.

Publisher's note: Springer Nature remains neutral with regard to jurisdictional claims in published maps and institutional affiliations.

References

1. Watson JD, Crick FHC. Molecular structure of nucleic acids: a structure for deoxyribose nucleic acid. Nature. 1953;171:737–8.
2. Bella J, Eaton M, Brodsky B, Berman HM. Crystal and molecular structure of a collagen-like peptide at 1.9 Å resolution. Science. 1994;266:75–81.
3. Shoulders MD, Raines RT. Collagen structure and stability. Ann Rev Biochem. 2009;78:929–58.
4. Plosky B. The nucleus: express yourself. Cell . 2013;152:1203–5.
5. Wu HCH, Sarko A. The double-helical molecular structure of crystalline B-amylose. Carbohydr Res. 1978;61:7–25.
6. Rappenecker G, Zugenmaier P. Detailed refinement of the crystal structure of V_h-amylose. Carbohydr Res. 1981;89:11–19.
7. Takahashi Y, Kumano T, Nishikawa S. Crystal structure of B-amylose. Macromolecules. 2004;37:6827–32.
8. Fukuhara G, Nakamura T, Yang C, Mori T, Inoue Y. Dual chiral, dual supramolecular diastereodifferentiating photocyclodimerization of 2-anthracenecarboxylate tethered to amylose scaffold. Org Lett. 2010;12:3510–3.
9. Shoda S, Uyama H, Kadokawa J, Kimura S, Kobayashi S. Enzymes as green catalysts for precision macromolecular synthesis. Chem Rev. 2016;116:2307–413.
10. Cellulose and cellulose derivatives special issue. Macromol Chem Phys 2000;201:1913–2100.
11. Fukuhara G, Nakamura T, Yang C, Mori T, Inoue Y. Diastereodifferentiating photocyclodimerization of 2-anthracenecarboxylate tethered to cellulose scaffold. J Org Chem. 2010;75:4307–10.
12. Foster EJ, Moon RJ, Agarwal UP, Bortner MJ, Bras J, Camarero-Espinosa S, et al. Current characterization methods for cellulose nanomaterials. Chem Soc Rev. 2018;47:2609–79.
13. Wohlhauser S, Delepierre G, Labet M, Morandi G, Thielemans W, Weder C, et al. Grafting polymers from cellulose nanocrystals: synthesis, properties, and applications. Macromolecules. 2018;51:6157–89.
14. Boraston AB, Bolam DN, Gilbert HJ, Davies GJ. Carbohydrate-binding modules: fine-tuning polysaccharide recognition. Biochem J. 2004;382:769–81.
15. Numata M, Shinkai S. Self-assembled polysaccharide nanotubes generated from β-1,3-glucan polysaccharides. Adv Polym Sci. 2008;220:65–121.
16. Shen J, Okamoto Y. Efficient separation of enantiomers using stereoregular chiral polymers. Chem Rev. 2016;116:1094–138.
17. Yanaki T, Norisuye T, Fujita H. Triple helix of *Schizophyllum commune* polysaccharide in dilute solution. 3. Hydrodynamic properties in water. Macromolecules. 1980;13:1462–6.
18. Deslandes Y, Marchessault RH, Sarko A. Triple-helical structure of (1 → 3)-β-D-glucan. Macromolecules. 1980;13:1466–71.
19. Stokke BT, Elgsaeter A, Brant DA, Kitamura S. Supercoiling in circular triple-helical polysaccharides. Macromolecules. 1991;24:6349–51.
20. Sakurai K, Uezu K, Numata M, Hasegawa T, Li C, Kaneko K, et al. β-1,3-Glucan polysaccharides as novel one-dimensional hosts for DNA/RNA, conjugated polymers and nanoparticles. Chem Commun. 2005;4383–98.
21. Numata M, Shinkai S. 'Supramolecular wrapping chemistry' by helix-forming polysaccharides: a powerful strategy for generating diverse polymeric nano-architectures. Chem Commun. 2011;47:1961–75.
22. Zhang Y, Kong H, Fang Y, Nishinari K, Phillips GO. Schizophyllan: a review on its structure, properties, bioactivities and recent developments. Bioact Carbohydr Diet Fibr. 2013;1:53–71.
23. Suzuki T, Hosono A, Hachimura S, Suzuki T, Kaminogawa S. Modulation of cytokine and immunogloblin a release by beta-(1,3-1,6)-glucan from *Aureobasidium pullulans* strain 1A1. Anim Cell Tech. 2006;14:369–75.
24. Kimura Y, Sumiyoshi M, Suzuki T, Sakanaka M. Antitumor and antimetastatic activity of a novel water-soluble low molecular weight β-1,3-D-glucan (branch β-1,6) isolated from *Aureobasidium pullulans* 1A1 strain black yeast. Antican Res. 2006;26:4131–42.
25. Suzuki T, Nakamura S, Nishikawa K, Nakayama S, Suzuki T. Production of highly purified β-glucan from *Aureobasidium pullulans* and its characteristics. Food Funct. 2006;2:45–50.
26. Kimura Y, Sumiyoshi M, Suzuki T, Suzuki T, Sakanaka M. Effects of water-soluble low-molecular-weight β-1,3-D-glucan (branch β-1,6) isolated from *Aureobasidium pullulans* 1A1 strain black yeast on restraint stress in mice. J Pharm Pharmcol. 2007;59:1137–44.
27. Kimura Y, Sumiyoshi M, Suzuki T. Protective effects of water-soluble low-molecular-weight β-(1,3-1,6)D-glucan purified from *Aureobasidium pullulans* GM-NH-1A1 against UFT toxicity in mice. J Pharm Pharmcol. 2009;61:795–800.
28. Fukuhara G, Inoue Y. Oligosaccharide sensing with chromophore-modified curdlan in aqueous media. Chem Commun. 2010;46:9128–30.
29. Fukuhara G, Imai M, Yang C, Mori T, Inoue Y. Enantiodifferentiating photoisomerization of (*Z*,*Z*)-1,3-cyclooctadiene included and sensitized by naphthoyl-curdlan. Org Lett. 2011;13:1856–9.
30. Fukuhara G, Sasaki M, Numata M, Mori T, Inoue Y. Oligosaccharide sensing in aqueous media by porphyrin-curdlan conjugates: a prêt-á-porter rather than haute-couture approach. Chem Eur J. 2017;23:11272–8.
31. Sasaki M, Ryoson Y, Numata M, Fukuhara G. Oligosaccharide sensing in aqueous media using porphyrin-curdlan conjugates: an allosteric signal-amplification system. J Org Chem. 2019;84:6017–27.
32. Fukuhara G, Inoue Y. Highly selective oligosaccharide sensing by a curdlan-polythiophene hybrid. J Am Chem Soc. 2011;133:768–70.
33. Fukuhara G, Imai M, Fuentealba D, Ishida Y, Kurohara H, Yang C, et al. Electrostatically promoted dynamic hybridization of glucans with cationic polythiophene. Org Biomol Chem. 2016;14:9741–50.
34. Harada N, Suzuki S, Uda H, Nakanishi K. Studies of the aromatic chirality method. The optical rotatory powers of di- and tribenzoate systems. J Am Chem Soc. 1971;93:5577–9.
35. Berova N, Bari LD, Pescitelli G. Application of electronic circular dichroism in configurational and conformational analysis of organic compounds. Chem Soc Rev. 2007;36:914–31.
36. Numata M, Kinoshita D, Hirose N, Kozawa T, Tamiaki H, Kikkawa Y, et al. Controlled stacking and unstacking of peripheral chlorophyll units drives the spring-like contraction and expansion of a semi-artificial helical polymer. Chem Eur J. 2013;19:1592–8.